HHS Public Access

Author manuscript

Neuroimage Rep. Author manuscript; available in PMC 2023 November 01.

Published in final edited form as:

Neuroimage Rep. 2023 September ; 3(3): . doi:10.1016/j.ynirp.2023.100179.

White matter microstructural integrity continues to develop from adolescence to young adulthood in mice and humans: Same phenotype, different mechanism

David J. Piekarski[a,*], **Natalie M. Zahr**[a,b], **Qingyu Zhao**[b], **Uran Ferizi**[a,b], **Kilian M. Pohl**[b], **Edith V. Sullivan**[b], **Adolf Pfefferbaum**[a,b]

[a]Center for Health Science, SRI International, 333 Ravenswood Ave., Menlo Park, CA, 94015, USA

[b]Department of Psychiatry and Behavioral Sciences, Stanford University School of, Medicine, 401 Quarry Rd., Stanford, CA, 94305, USA

Abstract

As direct evaluation of a mouse model of human neurodevelopment, adolescent and young adult mice and humans underwent MR diffusion tensor imaging to quantify age-related differences in microstructural integrity of brain white matter fibers. Fractional anisotropy (FA) was greater in older than younger mice and humans. Despite the cross-species commonality, the underlying developmental mechanism differed: whereas evidence for greater axonal extension contributed to higher FA in older mice, evidence for continuing myelination contributed to higher FA in human adolescent development. These differences occurred in the context of species distinctions in overall brain growth: whereas the continued growth of the brain and skull in the murine model can accommodate volume expansion into adulthood, human white matter volume and myelination continue growth into adulthood within a fixed intracranial volume. Appreciation of the similarities and differences in developmental mechanism can enhance the utility of animal models of brain white matter structure, function, and response to exogenous manipulation.

Keywords

Adolescence; Development; Diffusion tensor imaging; Human; Mouse; Translational

*Corresponding author: david@lorentz.bio (D.J. Piekarski).

Author contributions

Conceptualization: DJP, NMZ, AP, EVS; Methodology: DJP, NMZ, QZ, KMP, UF, AP, EVS; Formal statistical analysis: AP; Data Acquisition: DJP; Data Processing and curation: AP, QZ, KMP, UF; Writing-original draft preparation: DJP, AP, EVS; Writing-review and editing: DJP, NMZ, QZ, KMP, UF, AP, EVS; Funding acquisition: AP, NMZ, KMP, EVS, QZ.

Declaration of competing interest

The authors declare that they have no known competing financial interests or personal relationships that could have appeared to influence the work reported in this paper.

The authors have no competing interests to disclose.

1. Introduction

Animal models of human behavior, physiology, and development are invaluable for discovering basic biological mechanisms, testing safety and efficacy of pharmacological agents, and identifying biological effects of environmental toxins (Mirsalis, 1995). While it is often acknowledged that differences between species may limit translation of results to the human condition, relatively few studies explicitly aim to determine an animal model's translational relevance. This shortcoming is exemplified in neuroscience research in which human and animal experiments are most often conducted in non-overlapping domains, using different techniques and approaches that yield fundamentally different datasets, often across different neural scales. Human neuroscience is typically limited to non-invasive approaches and therefore is dominated by techniques such as magnetic resonance imaging (MRI), magnetoencephalography, or electrophysiology, which measure aggregate effects over tens of thousands of cells. On the other hand, experiments in animal models commonly use invasive approaches that exquisitely detail experimental effects in numerable cells, with manipulations unavailable in human studies. These different analysis levels yield an explanatory gap that hinders accurate translation from animal to human mechanisms (Barron et al., 2021).

Bridging this gap requires application of the same research tools and methods to multiple species to determine generalizability of effects and to aid in the synthesis of non-overlapping data to aid interpretation of results in each species (Barron et al., 2021). Herein we apply non-invasive MRI to study the development of white matter microstructure during adolescent development in mice and humans to address this explanatory gap and to identify species similarities and differences in brain-wide white matter neurodevelopment.

In humans, postpartum brain development continues through adolescence with decelerating yet significant growth into young adulthood (Bethlehem et al., 2022; Giedd et al., 1999; Slater et al., 2019; Sowell et al., 2004). Trajectories of adolescent brain volume change are heterosynchronous and differ by tissue type, where gray matter volumes, representing neurons, glia, and neuropil, increase until about age 10–12 years followed by continuous decline thereafter (Bethlehem et al., 2022; Kennedy et al., 2009; Pfefferbaum et al., 2013). By contrast, white matter volumes, composed of glia, axons, and myelin, expand from birth with a decelerating rate of growth in late adolescence to early adulthood (Lebel and Deoni, 2018; Lenroot et al., 2007; Pfefferbaum et al., 2016). In the early years of development, these expanding volumes coincide with the expanding intracranial vault, which reaches a maximum before 15 years of age (Dekaban and Sadowsky, 1978), and therefore limits brain growth beyond this age. As such, white matter growth is complementary to gray matter volume declines (Bethlehem et al., 2022; Giedd et al., 1999; Lebel and Beaulieu, 2011). Brain regions undergoing these growth dynamics are rendered especially sensitive to and altered by environmental factors, such as early life stressors or exposure to neurotoxic substances (Drzewiecki and Juraska, 2020; Pfefferbaum et al., 2000, 2001, 2004; Sullivan et al., 2001). Thus, prior to modeling a stressor's influence on the brain during adolescent development, the patterns of normal neurodevelopment with respect to age, pubertal stage, and sex as moderators of growth trajectories must be established.

In vivo human studies have tracked the development of white matter microstructure using magnetic resonance diffusion tensor imaging (DTI) in cross-sectional (Asato et al., 2010; Pohl et al., 2016) and longitudinal (Lebel and Beaulieu, 2011; Simmonds et al., 2014) studies. Myelin continues to develop into middle age (Beck et al., 2021; Kiely et al., 2022; Westlye et al., 2010; Yeatman et al., 2014) and begins its decline at significantly later ages than gray matter volume decline (Bethlehem et al., 2022; Giedd et al., 1999; Pfefferbaum et al., 2016, 2018). Although sex differences in developmental trajectories of white matter microstructure (Bava et al., 2011; Lebel et al., 2010; Schmithorst et al., 2008) may be influenced by gonadal hormones at puberty (Herting et al., 2012; Ho et al., 2020), sex differences in white matter DTI metrics are largely attenuated in post-pubertal adulthood (Karlsgodt et al., 2015; Sullivan et al., 2010; Tamnes et al., 2010).

Less attention has been paid to neuroimaging metrics of white matter than gray matter development in model species, but studies that do focus on white matter largely employ invasive, postmortem analyses of cellular and molecular white matter measures. Such studies have identified white matter differences causally associated with age, sex, and pubertal hormones, suggesting that white matter plasticity in these species slows with advancing age, but persists, at least into young adulthood (Bimonte et al., 2000; Koss et al., 2015; Mack et al., 1993; Markham et al., 2007) as observed in human studies. Although these approaches leverage unique benefits of model species, they tend to focus solely on one or a few specific brain regions and therefore do not provide a representation of whole brain dynamics during times of continuing growth.

Differences between rodent and human brains in distribution of gray vs. white matter and growth patterns may indicate limitations in directly translating neurodevelopmental insights from various rodent models to humans. Among the salient morphological differences between large, gyrencephalic and small, lissencephalic brains is their proportion of gray-to-white matter volume (Ventura-Antunes et al., 2013; Zhang and Sejnowski, 2000), where rodents may have 80% gray matter and 20% white matter, whereas humans have the reverse proportion, driven by the need for long-range connectivity across the expanded cortex (Zhang and Sejnowski, 2000).

Because mice are the most widely used non-human subjects in biomedical research (Carbone, 2021), we investigated translatability of white matter development between mice and humans by conducting cross-sectional DTI studies in adolescent and young adult cohorts of male and female mice with parallel comparison of adolescent and young adult humans who were comparable in age and sex to the mouse groups (Dutta and Sengupta, 2016; Piekarski et al., 2017b) and had undergone DTI as participants in the National Consortium on Alcohol and NeuroDevelopment in Adolescence (NCANDA) study (Brown et al., 2015; Pfefferbaum et al., 2016; Pohl et al., 2016; Zhao et al., 2021). These data demonstrate that mice and humans undergo both parallel and divergent white matter microstructural changes during adolescent development and suggest that developmental insights into adolescent changes in white matter tracts should be interpreted with caution and appropriate nuance.

2. Methods

All experimental procedures with mice were conducted in accordance with the Guide for the Care and Use of Laboratory Animals of the National Institutes of Health. The Institutional Animal Care and Use Committees at SRI International and Stanford University approved all procedures. Human participants underwent informed consent processes with a research associate trained in human subject research protocols. Adult participants or the parents of minor participants provided written informed consent before starting the study; minor participants provided assent. The Institutional Review Boards of each data collection site and the NCANDA oversight committee approved this study.

2.1. Mouse study

2.1.1. Descriptions and procedures—C57Bl/6j mice, acquired from the Jackson Laboratories (Sacramento, CA), included 15 peri-pubertal (7 female) and 24 adult (16 female) mice. Baseline weights were as follows: adolescent females = 15.71 ± 0.27 g; adolescent males = 17.35 ± 0.43 g; adult females = 22.32 ± 0.38 g; adult males = 30.93 ± 0.62 g. Mice were housed 4 per cage, maintained in a pathogen-free facility on a 12-hr light/dark cycle, and had ad libitum access to regular chow and water. Following at least one week of acclimation to the vivarium, each mouse underwent MR scanning at postnatal day (P) 29–30 for the adolescent group [approximate start of puberty (Piekarski et al., 2017a)] and P104-129 for the adult group.

2.1.2. MRI and DTI acquisition—MR data were collected on a Bruker 70/16 US AVANCE III 7.0T system (Karlsruhe, Germany) with 380 mT/m gradient strength on each (X, Y, and Z) axis, slew rate of 3420 T/m/s, 16 cm bore size, and ParaVision 6.1 software. Before each scan, animals were anesthetized with isoflurane (3% for induction; ~0.5–2% for maintenance) and body weight was acquired. Animals were then placed on an animal cradle base with built-in water circulation for body temperature control. Respiration was monitored throughout each ~1hr scan. All animals received subcutaneous saline (0.9%) for hydration at the end of the scan (0.5 cc).

A mouse head volume coil (23 mm) was used to acquire a gradient-recalled echo (GRE) localizer scan used to position the animals in the scanner and for graphical prescription of the subsequent scans. Structural analysis was based on acquisition of T2-weighted, high-resolution, TurboRare sequences: repetition time (TR) = 6774.8ms; echo time (TE) = 33ms; field of view (FOV) = 16 × 16 matrix = 128 × 64; pixel size = 0.125 × 0.25 × 0.25 mm; 4 averages; echo spacing = 11ms; rare factor (i.e., echo train length) = 8; slice thickness = 0.25 mm; 65 slices. The data were reformatted to 0.125 mm isotropic voxels for analysis. DTI echoplanar data acquisition parameters were TR = 3000ms; TE = 29.14ms; FOV = 16 mm; matrix = 100 × 50; 0.16 mm in x and 0.32 mm in y (phase encode); slice thickness = 0.32 mm; 56 slices; diffusion gradient duration was 5 msec and amplitude was 66.414 mT/m. The data were reformatted with linear interpolation to 0.16 mm isotropic voxels for analysis. One data set include six 3-D frames of b = 0, and one set of 36 directions of b = 1000. A second data set with 6 directions of b = 1000 with reversed readout polarity was used for echoplanar spatial distortion correction.

2.1.3. DTI analysis: tract-based spatial statistics (TBSS)—In subject space, FSL "topup" (Jenkinson et al., 2012; Smith et al., 2004) was used to minimize echoplanar spatial distortion. FSL "dtifit" was used to create the tensors and extract DTI metrics: fractional anisotropy (FA), mean diffusivity (MD), axial diffusivity (AD), and radial diffusivity (RD). Native FA images were upsampled into laboratory atlas space by non-rigidly registering b0 to the T2 scan and then registering T2 to an atlas with 0.2 mm 3D isotropic resolution.

Each upsampled FA image was further registered to an average mouse FA template constructed from all adolescent mice FA images. After registration, TBSS contrasts were performed first testing for sex effects among the adolescent and adult animals separately and then contrasting the adolescent-vs-adult mice (Smith et al., 2004). The TBSS FA analysis procedure included the standard skeleton generation (44, 324 voxels) and randomization testing with 5000 permutations. Two-tailed statistical testing was done with cluster-based thresholding corrected for multiple comparisons by using the null distribution of the maximum (across the image) cluster mass ("FWE-corrected" procedure). The underlying diffusion metrics - MD, AD, and RD - were also generated for the whole FA skeleton and subjected to adolescent-vs-adult contrast testing identical to that of FA. Finally, to explicate the underlying mechanism of FA differences, the mean FA, MD, AD and RD values of each cluster where FA was greater for adults than adolescents were tested for group differences between adults and adolescents with Welch Two Sample t-tests.

2.1.4. Brain tissue volumes—We quantified white matter volumes directly using T2-weighted RARE images. As previously reported (Piekarski et al., 2022) wherein a registration-based segmentation approach used 15 mouse brains registered to each other to form a template brain followed by intensity thresholding to define a gray matter, white matter, and CSF laboratory mouse atlas. Each of the brains of this study was segmented by non-rigidly registering the template to the animal's T2 and transforming the atlas to the animal's native T2 space. The resulting label map identified the major white matter tracts—the corpus callosum, anterior commissure, and hippocampal fimbria. Brain volume was the sum of volumes of the three tissue types.

2.2. Human study

2.2.1. Participant description—We obtained data from the NCANDA, a multi-site study designed to track the trajectories of regional brain development during a time of high risk for initiating alcohol consumption. A full description of the NCANDA recruitment strategies, sample, and demographics appear elsewhere (Brown et al., 2015; Pfefferbaum et al., 2016). Data for this project were taken from the public data release NCANDA_PUBLIC_7Y_DIFFUSION_V01 and limited to data collected from the 3 sites (SRI International, UC San Diego, Duke University) that used GE scanners (to simplify data harmonization).

Adolescent and young adults were selected from the NCANDA database to approximate the age and sex distribution of the mice. Only participants meeting criteria as no-to-low alcohol drinkers (Pfefferbaum et al., 2016) and without structural anomalies (Sullivan et al., 2017) were included; only one scan from each participant was included. Accordingly,

this analysis used all available data of participants who met these criteria from the two age groups: 31 male and 31 female participants, ages 12.0–12.9 years, and 38 male and 43 female participants, 20.0–20.9 years (Table 1).

2.2.2. MRI and DTI acquisition—MR data were acquired on GE whole body 3T systems. Diffusion-Weighted Image (DWI) acquisition was a 2D Axial Spin Echo, Echo-Planar protocol with two b = 0/1000 and 60 directions (Acquisition Time: 8 m 24s) as well as a reverse-phase acquisition of the 2D Axial Spin Echo-Planar protocol (Acquisition Time: 1 m 12s) with b = 0/500 and 6 directions (TR = 10,000ms, TE = 85ms, Thick = 2.5 mm, Number of Slices = 64, FOV = 24 cm, xy_matrix = 96, Phase = A/P, Partial k-space (48/64), Acceleration = 2, Resolution = 2.5 × 2.5 × 2.5 mm, Fat Sat = on; diffusion gradient duration was 19.8msec and amplitude was 49.01 mT/m).

The structural and diffusion data of all NCANDA participants were preprocessed using the publicly available longitudinal NCANDA pipeline (Pfefferbaum et al., 2018). Skull stripping and aligning with the SRI 24 atlas (Rohlfing et al., 2010) were performed by registering the T1 data to the atlas with ANTS (Avants et al., 2011). The b0 scan of the DTI sequence was aligned to the T1 MRI by aligning the b0 to the T2 scan via ANTS and aligning the T2 to the T1 via CMTK (Rohlfing and Maurer, 2003). In addition to skull stripping, the pipeline performed removal of bad single shots, pepolar echo-planar structural distortion, eddy-current distortion correction and computation of the four DTI metrics: FA, MD, AD, and RD.

2.2.3. DTI analysis: TBSS—Adolescent and young adult FA, MD, AD and RD data that were previously registered to a standard lab template (Rohlfing et al., 2010) were used for TBSS analysis. The TBSS FA analysis procedure was the same as that for the mice including the standard skeleton generation (162,204 voxels), randomization testing with 5000 permutations, cluster-based thresholding corrected for multiple comparisons, and testing group difference. As with the mice, the underlying diffusion metrics - MD, AD, and RD - were also generated for the whole FA skeleton and subjected to adolescent-vs-adult contrast testing identical to that of FA. Finally, to explicate the underlying mechanism of FA differences, the mean FA, MD, AD and RD values of each cluster where FA was greater for adults than adolescents were tested for group differences between adults and adolescents with Welch Two Sample t-tests.

From the voxels that differed in FA between adolescents and young adults, a general linear model (*glm*) conducted with R tested the potential independent contributions of sex, site, and ethnicity to age group differences in FA using the mean FA of each participant.

2.2.4. Brain tissue volumes—NCANDA brain volume measures were generated from the NCANDA pipeline (Pfefferbaum et al., 2018). Specifically, the pipeline performed for both T1w and T2w MRI noise removal and image inhomogeneity correction. The pipeline then aligned the T2w MRI to the T1w MRI and the skull stripped and non-rigid aligned the T1w MRI to the SRI24 atlas (Rohlfing et al., 2010). Guided by the atlas, tissue segmentation (gray matter, white matter, and cerebrospinal fluid) was performed via Atropos (Avants et al., 2011). The resulting label map was used to determine the volume of those three brain

compartments and the ICV was the sum of all voxels segmented as gray matter, white matter, and CSF in the supratentorial space.

3. Results

Parallel diffusion tensor imaging experiments were conducted on young adolescent and young adult mice (P29–30 vs P104–129) and humans (12–12.9 years vs 20–20.9 years) of both sexes. Results are presented first for the mouse and then for human comparisons of white matter DTI metrics and imaging estimates of intracranial volume (ICV) and white matter volume.

3.1. Mouse study

3.1.1. Age differences in DTI metrics for the whole white matter skeleton

—The adolescent-vs-adult FA contrast produced 6 significant clusters ($p < 0.05$ FWE-corrected) totaling 7395 voxels (7 in the smallest and 6776 in the largest), where adults had higher FA than adolescents (Fig. 1). No significant clusters were identified where adolescents had higher FA than adults. No sex differences were identified in any FA clusters in either adolescent or adult mice ($p > 0.05$).

Age differences in diffusivity metrics were tested on the entire FA skeleton. For each of the three diffusivity metrics, the adolescent-vs-adult contrasts identified 1 significant cluster ($p < 0.05$ FWE-corrected) of higher diffusivity in the adults than in the adolescents; in no case did adolescents have greater diffusivity than adults. The mean diffusivity (MD) contrast produced a significant cluster containing 30,871 voxels, the axial diffusivity (AD) cluster contained 31,648 voxels, and the radial diffusivity (RD) cluster contained 26,882 voxels.

Diffusivity metrics were assessed in the voxels showing age differences in FA. Group statistics (N, mean, SD) are presented in Table 2, and histograms (Fig. 2) display distributions of each DTI metric by age group. Mean FA was 18.76% higher in adults than adolescents (t (20.554) = 10.057, p = 2.182e-09) as was mean MD, which was 6.91% higher in adults than adolescents (t (35.391) = 5.222, p = 7.948e-06). Mean AD was significantly higher in adults than adolescents by 13.30% (t (33.094) = 10.873, p = 1.842e-12), whereas mean RD did not differ between the age groups in the FA-identified regions (t (34.688) = 1.2923, p = 0.205).

3.1.2. Volume difference between adolescents and adults—

Total brain volume was 13.1% larger in the adult (489.4 mm^3) than adolescent mice (432.9 mm^3) (t (35.45) = −9.9101, p = 9.343e-12). Using the segmentation approach, across the combined groups of adolescent and adult mice, there was a significant correlation between white matter volume and brain volume (r = 0.735, p = 4.476e-08).

Native brain white matter volume was significantly smaller in adolescents than adults (6.710 vs 9.352 mm^3, t = −16.738, p-value <2.2e-16). Brain volume-controlled values were also created by regression analysis across all animals and continued to show significantly smaller white matter volume in adolescents (7.742 vs 8.757 mm^3, t = −4.1575, p-value = 0.000178).

General linear model regression (*lm* R) of white matter as a function of brain volume + age produced significant effect of age (t = 8.187, p = 6.49e-10) but not brain volume (t = 0.924, p = 0.3615) indicating a significant difference in white matter volume between adolescents and adult mice irrespective of brain volume.

3.2. Human study

3.2.1. Age differences in DTI metrics for the whole white matter skeleton—

The adolescent-vs-adult FA contrast produced 4 clusters totaling 51,722 voxels (17 in the smallest and 50,436 in the largest) with adults having higher FA than adolescents (Fig. 2, FA). No significant clusters were identified in which adolescents had higher FA than adults, and no clusters met $p < 0.05$ significance for sex differences in FA within the adolescents or adults. The *glm* used to test whether the group differences in FA were attributable to sex, site, or ethnicity yielded a significant overall effect (F (5,137) = 18.65, p = 4.2e-14) with only the age group showing a significant effect (t = 9.223, p = 4.65e-16).

Age differences in diffusivity metrics were tested on the entire FA skeleton. The adolescent-vs-adult MD contrast produced 1 cluster with 105,067 voxels where adults had lower MD than adolescents. For AD, the adolescent-vs-adult contrast produced 3 clusters totaling 66,670 voxels (35 in the smallest and 66,293 in the largest) where adults had lower AD than adolescents. For the adolescent-vs-adult RD contrast, 1 cluster of 94,986 voxels indicated that adults had lower RD than adolescents. No significant clusters were identified in which adolescents had higher FA, MD, or AD than adults. Group differences for FA and the underlying diffusion metrics where FA was greater in adults than adolescents are presented in Table 2, where histograms (Fig. 2) display distributions of each DTI metric by age group.

Mean FA was 4.30% **higher** in the adults than adolescents (t (125.1) = 8.9174, p = 4.855e-15). Mean MD was 2.01% **lower** in adults than adolescents (t (136.4) = −6.2301, p = 5.416e-09). AD did not differ between the ages, showing only a −0.22% difference (t (136.31) = −0.8041, p = 0.3802), whereas mean RD did show a group difference, where the RD in the adults was 3.85% **lower** than that in the adolescents (t (132.32) = −7.9778, p = 6.227e-13).

3.2.2. Volume difference between adolescents and adults—

Whole-brain volume was non-significantly larger in the adolescents (1331.1 cm^3) than adults (1297.0 cm^3) (t (119.14) = 1.438, p = 0.1531) (Fig. 3D). Total supratentorial white matter volume did not differ between the adults (443.2 cm^3) and adolescents (436.4 cm^3) (t (118.29) = −0.7682 p = 0.4439) (Fig. 3E).

Because total white matter volume and ICV were highly correlated (r = 0.899, p = 2.2e-16) (Fig. 3, bottom middle), white matter volumes were regressed on ICV. The regression analysis adjusting for ICV resulted in a significant group difference (t (129.42) = −5.225, p = 6.779e-07), where the adults had larger white matter volumes (448.2 cm^3) than the adolescents (429.8 cm^3) (Fig. 3F).

4. Discussion

This whole-brain survey of white matter microstructure using DTI revealed higher FA in young adults than adolescents in both mice and humans. These age-related differences provide in vivo evidence for continued neurodevelopment in white matter fiber orientational organization and axonal packing well beyond adolescence. FA is a measure of linearity in the diffusion of water within a voxel, which is a composite of the effects of RD and AD. Despite the commonality of higher FA in older mice and humans, the underlying diffusivity indices differed between species: AD drove age differences in FA in mice, whereas RD drove FA differences in humans.

DTI studies of human adolescents and young adults report developmental plateaus by age 18–20 (Pohl et al., 2016; Sousa et al., 2018). Longitudinal tractography revealed that FA increased over a 1–6 year interval in youth and young adults ages 5–32 years (Lebel and Beaulieu, 2011). Although differences in developmental trajectories were noted across fiber systems, overall the increases in FA were accompanied by declines in RD (Lebel and Beaulieu, 2011), which is commonly interpreted as evidence for increasing myelination and axonal packing (Beaulieu, 2002; Song et al., 2005). In contrast to humans, FA increases in mice were associated with greater AD, which is thought to be a marker of axonal coherence (Song et al., 2003) and elongation (Gao et al., 2009). This pattern of development has also been reported in the corpus callosum of human youth (Lebel and Beaulieu, 2011).

Species differences in mechanisms underlying FA development may relate to differences in overall brain growth and cranial plasticity patterns that differently constrain or enable continued neurodevelopment. As noted, human brain volume reaches its maximum in early adolescence and thus developmental increases in white matter volume must be accompanied by concomitant decreases in other tissues, observed as declining gray matter (Bethlehem et al., 2022; Giedd et al., 1999; Pfefferbaum et al., 2016; Sowell et al., 2004). In rodents, by contrast, longitudinal MRI studies report continued whole-brain growth well into adulthood (Sullivan et al., 2006), with both gray matter and white matter volumes increasing. Wistar P rats imaged repeatedly over 12 months from young (P88) to mid-adult (P452) ages showed brain growth of 10%, reaching asymptote by age 284 days (Sullivan et al., 2006). A similar effect was observed in Fisher 344 rats (Zahr et al., 2021). C57BL/6 mice also show prolonged periods of brain growth, with cross-sectional increases of ~12% brain volume between groups imaged during early adolescence (P35) and early adulthood (P116) (Piekarski et al., 2022). Given that mouse brain volume growth may cease by early adulthood (Hammelrath et al., 2016; Piekarski et al., 2022), this effect may have occurred during adolescent or young adult.

These effects may be related to fundamental differences in cranial plasticity that permit continued brain volume expansion in rodents. The development of the brain, skull, and cranial sutures is a complex process coordinated by a number of intercellular signaling molecules that pair calvarial growth with fusion timing to allow for brain expansion (Liu et al., 1995) during development. While the human intracranial vault becomes fixed during the second decade of life (Dekaban and Sadowsky, 1978; White et al., 2021; Wilkinson et al., 2020), the murine skull remains plastic well-into adulthood (Zhang et al., 2013),

which permits continued brain expansion in adult rodents. These effects may explain the coordinated adolescent gray matter declines and white matter expansion of human neurodevelopment that are absent in rodents. Given that adolescent and adult rodents do not show widespread neurogenesis outside of the select few neural regions (Blankers and Galea, 2021), it is possible that the extended growth phase in rodents may be accompanied by extension of axons, which is reflected in the noted increases in axial diffusivity with age. This observation is consistent with an earlier report that found continued growth of the volume and length of the corpus callosum in the P rats (Sullivan et al., 2006). By contrast, the decrease in RD with age in humans is consistent with increasing myelination, which continues to develop into the third and even fourth decade of life (Beck et al., 2021; Jernigan and Stiles, 2017; Westlye et al., 2010; Yeatman et al., 2014).

Mice show similar patterns of myelination to those inferred in humans from DTI studies. In mice, white matter tracts continue to be myelinated well into adulthood, with the rate of myelination declining after adolescence (Sturrock, 1980). Nonetheless, numerous studies demonstrate that myelin continues to be laid down, and its structural charactersitics continue to change throughout mid life, before declining in old age (Hill et al., 2018; Safaiyan et al., 2016), which mimics human lifetime white matter patterns Giorgio et al., 2008, 2010). Thus, while mice appear to demonstrate broadly uniform myelination trajectories across the lifespan, the continued growth in overall brain volume, paired with axonal elongation, may reduce changes in myelin related RD metrics even in the context of increasing myelination.

In vivo measurements of myelin are, at best, estimates. For a generation, DTI metrics, notably radial diffusivity, have been considered accepted approximations of myelin, for example, validated by studies comparing in vivo DTI with ex vivo histology in mice (Song et al., 2003). More recently, additional in vivo MRI metrics have been developed to account for the contaminating presence of free water in the myelin compartment. Among these developments is the myelin water fraction (MWF), which requires acquisition of multiple T2-wt echoes to model the T2 relaxation time signal decay that reflects water content in the peri-axonal spaces. Removal of this contaminating water signal from the tissue signal yields a cleaner estimate of the target tissue, in this case, myelin. Using MWF, Arshad et al. (2016) challenged the accuracy of RD from DTI (uncorrected for presence of free water) in modeling myelin development and aging. Accordingly, they tested their hypothesis that accurate modeling of normal myelin development and aging would follow an inverted U-shaped function (predicted from postmortem cases) rather than a linear age function and compared myelin estimates from MWF with those from DTI in healthy adult men and women, age 18–84 years old. These cross-sectional myelin estimates supported their hypothesis in showing that the MWF estimates were curvilinear (U-shaped), whereas the DTI estimates were linear across their 76-year age range. The implications of these findings for the current study highlight a salient limitation herein of the lack of multiple T2 echoes that were required for calculation of MWF estimates. Critically, the age range of the current study spanned only the youngest age range of the Arshad et al. (2016) study and could only be modeled as linear.

Despite the strengths of the present study, its limitations must be acknowledged. Specifically, although the non-invasive feature of MRI enables safe, longitudinal data

collection, the present study used only cross-sectional data. Future longitudinal analyses with multiple timepoints should be conducted to allow a more nuanced approach to aligning neurodevelopmental trajectories between species, including potential transient effects of biological sex that may be present during active adolescent development but then dissipate in young adulthood. The present data also rely solely on DTI data to identify species differences in neurodevelopment, which is a biological process. As such, strong conclusions about the biological mechanism driving these differences are not possible without follow-up, histological studies of brain tissue constituents. Finally, the present study did not parse the effects by white matter region, which will limit identification of regional differences in brain development that may vary between species.

5. Conclusion

These species-related disparities in brain growth patterns and endpoints suggest translational limitations regarding rodent models of human neurodevelopment. When conducting research aimed at translating between animal models and humans, these differences need consideration when selecting the age or neurodevelopmental timepoint for experimental interdictions or data collection. Appreciation of the differences between species paired with considered interpretation of the data will enhance validity of translational studies and ultimate confidence in biological insights drawn from model species.

Acknowledgment

Support for this project was provided by the NIAAA (AA005965, AA010723, AA028840) and NIDA (DA057567). The data were part of the public data release NCANDA_PUBLIC_7Y_DIFFUSION_V01,[1] distributed according to the NCANDA Data Distribution agreement[2] whose collection and distribution were supported by NIH funding AA021681, AA021690, AA021691, AA021692, AA021695, AA021696, AA021697.

Data availability

Data will be made available on request.

References

Arshad M, Stanley JA, Raz N, 2016. Adult age differences in subcortical melin content are consistent with protracted myelination and unrelated to diffusion tensor imaging indices. Neuroimage 143, 26–29. [PubMed: 27561713]

Asato MR, Terwilliger R, Woo J, Luna B, 2010. White matter development in adolescence: a DTI study. Cerebr. Cortex 20, 2122–2131. 10.1093/cercor/bhp282.

Avants BB, Tustison NJ, Cook PA, Gee JC, 2011. An open source multivariate framework for the n-tissue segmentation with evaluation of public data. Neuroinformatics 9, 381–400. [PubMed: 21373993]

Barron HC, Mars RB, Dupret D, Lerch JP, Sampaio-Baptista C, 2021. Cross-species neuroscience: closing the explanatory gap. Phil. Trans. R. Soc. B 376, 20190633. 10.1098/rstb.2019.0633. [PubMed: 33190601]

[1]Pohl, K.M., Sullivan EV, Baker FC, Brown SA, Clark DB, de Zambotti M, Goldston D, Luna B, Nagel BJ, Nooner KB, Tapert SF, Pfefferbaum A: The 'NCANDA_PUBLIC_7Y_DIFFUSION_V01′ Data Release of the National Consortium on Alcohol and NeuroDevelopment in Adolescence (NCANDA), Sage Bionetworks Synapse. https://doi.org/10.7303/syn43162820.

[2]https://www.niaaa.nih.gov/ncanda-data-distribution-agreement.

Bava S, Boucquey V, Goldenberg D, Thayer RE, Ward M, Jacobus J, Tapert SF, 2011. Sex differences in adolescent white matter architecture. Brain Res 1375, 41–48. 10.1016/j.brainres.2010.12.051. [PubMed: 21172320]

Beaulieu C, 2002. The basis of anisotropic water diffusion in the nervous system - a technical review. NMR Biomed 15, 435–455. 10.1002/nbm.782. [PubMed: 12489094]

Beck D, de Lange A-MG, Maximov II, Richard G, Andreassen OA, Nordvik JE, Westlye LT, 2021. White matter microstructure across the adult lifespan: a mixed longitudinal and cross-sectional study using advanced diffusion models and brain-age prediction. Neuroimage 224, 117441. 10.1016/j.neuroimage.2020.117441. [PubMed: 33039618]

Bethlehem RAI, Seidlitz J, White SR, Vogel JW, Anderson KM, Adamson C, Adler S, Alexopoulos GS, Anagnostou E, Areces-Gonzalez A, Astle DE, Auyeung B, Ayub M, Bae J, Ball G, Baron-Cohen S, Beare R, Bedford SA, Benegal V, Beyer F, Blangero J, Blesa Cábez M, Boardman JP, Borzage M, Bosch-Bayard JF, Bourke N, Calhoun VD, Chakravarty MM, Chen C, Chertavian C, Chetelat G, Chong YS, Cole JH, Corvin A, Costantino M, Courchesne E, Crivello F, Cropley VL, Crosbie J, Crossley N, Delarue M, Delorme R, Desrivieres S, Devenyi GA, Di Biase MA, Dolan R, Donald KA, Donohoe G, Dunlop K, Edwards AD, Elison JT, Ellis CT, Elman JA, Eyler L, Fair DA, Feczko E, Fletcher PC, Fonagy P, Franz CE, Galan-Garcia L, Gholipour A, Giedd J, Gilmore JH, Glahn DC, Goodyer IM, Grant PE, Groenewold NA, Gunning FM, Gur RE, Gur RC, Hammill CF, Hansson O, Hedden T, Heinz A, Henson RN, Heuer K, Hoare J, Holla B, Holmes AJ, Holt R, Huang H, Im K, Ipser J, Jack CR, Jackowski AP, Jia T, Johnson KA, Jones PB, Jones DT, Kahn RS, Karlsson H, Karlsson L, Kawashima R, Kelley EA, Kern S, Kim KW, Kitzbichler MG, Kremen WS, Lalonde F, Landeau B, Lee S, Lerch J, Lewis JD, Li J, Liao W, Liston C, Lombardo MV, Lv J, Lynch C, Mallard TT, Marcelis M, Markello RD, Mathias SR, Mazoyer B, McGuire P, Meaney MJ, Mechelli A, Medic N, Misic B, Morgan SE, Mothersill D, Nigg J, Ong MQW, Ortinau C, Ossenkoppele R, Ouyang M, Palaniyappan L, Paly L, Pan PM, Pantelis C, Park MM, Paus T, Pausova Z, Paz-Linares D, Pichet Binette A, Pierce K, Qian X, Qiu J, Qiu A, Raznahan A, Rittman T, Rodrigue A, Rollins CK, Romero-Garcia R, Ronan L, Rosenberg MD, Rowitch DH, Salum GA, Satterthwaite TD, Schaare HL, Schachar RJ, Schultz AP, Schumann G, Schöll M, Sharp D, Shinohara RT, Skoog I, Smyser CD, Sperling RA, Stein DJ, Stolicyn A, Suckling J, Sullivan G, Taki Y, Thyreau B, Toro R, Traut N, Tsvetanov KA, Turk-Browne NB, Tuulari JJ, Tzourio C, Vachon-Presseau É, Valdes-Sosa MJ, Valdes-Sosa PA, Valk SL, van Amelsvoort T, Vandekar SN, Vasung L, Victoria LW, Villeneuve S, Villringer A, Vértes PE, Wagstyl K, Wang YS, Warfield SK, Warrier V, Westman E, Westwater ML, Whalley HC, Witte AV, Yang N, Yeo B, Yun H, Zalesky A, Zar HJ, Zettergren A, Zhou JH, Ziauddeen H, Zugman A, Zuo XN, 3R-BRAIN, AIBL, Rowe C, Alzheimer's Disease Neuroimaging Initiative, Alzheimer's Disease Repository Without Borders Investigators, Frisoni GB, CALM Team, Cam-CAN, CCNP, COBRE, cVEDA, ENIGMA Developmental Brain Age Working Group, Developing Human Connectome Project, FinnBrain, Harvard Aging Brain Study, IMAGEN, KNE96, The Mayo Clinic Study of Aging, NSPN, POND, The PREVENT-AD Research Group, Binette AP, VETSA, Bullmore ET, Alexander-Bloch AF, 2022. Brain charts for the human lifespan. Nature 604, 525–533. 10.1038/s41586-022-04554-y. [PubMed: 35388223]

Bimonte HA, Mack CM, Stavnezer AJ, Denenberg VH, 2000. Ovarian hormones can organize the rat corpus callosum in adulthood. Dev. Brain Res 121, 169–177. 10.1016/s0165-3806(00)00043-2. [PubMed: 10876029]

Blankers SA, Galea LAM, 2021. Androgens and adult neurogenesis in the Hippocampus. Androgens: Clinical Research and Therapeutics 2, 203–215. 10.1089/andro.2021.0016. [PubMed: 35024692]

Brown SA, Brumback T, Tomlinson K, Cummins K, Thompson WK, Nagel BJ, De Bellis MD, Hooper SR, Clark DB, Chung T, Hasler BP, Colrain IM, Baker FC, Prouty D, Pfefferbaum A, Sullivan EV, Pohl KM, Rohlfing T, Nichols BN, Chu W, Tapert SF, 2015. The national Consortium on alcohol and NeuroDevelopment in adolescence (NCANDA): a multisite study of adolescent development and substance use. J. Stud. Alcohol Drugs 76, 895–908. 10.15288/jsad.2015.76.895. [PubMed: 26562597]

Carbone L, 2021. Estimating mouse and rat use in American laboratories by extrapolation from Animal Welfare Act-regulated species. Sci. Rep 11, 493. 10.1038/s41598-020-79961-0. [PubMed: 33436799]

Dekaban AS, Sadowsky D, 1978. Changes in brain weights during the span of human life: relation of brain weights to body heights and body weights. Ann. Neurol 4, 345–356. 10.1002/ana.410040410. [PubMed: 727739]

Drzewiecki CM, Juraska JM, 2020. The structural reorganization of the prefrontal cortex during adolescence as a framework for vulnerability to the environment. Pharmacol. Biochem. Behav 199, 173044 10.1016/j.pbb.2020.173044. [PubMed: 33035531]

Dutta S, Sengupta P, 2016. Men and mice: relating their ages. Life Sci 152, 244–248. 10.1016/j.lfs.2015.10.025. [PubMed: 26596563]

Gao W, Lin W, Chen Y, Gerig G, Smith JK, Jewells V, Gilmore JH, 2009. Temporal and spatial development of axonal maturation and myelination of white matter in the developing brain. AJNR Am J Neuroradiol 30, 290–296. 10.3174/ajnr.A1363. [PubMed: 19001533]

Giedd JN, Blumenthal J, Jeffries NO, Castellanos FX, Liu H, Zijdenbos A, Paus T, Evans AC, Rapoport JL, 1999. Brain development during childhood and adolescence: a longitudinal MRI study. Nat. Neurosci 2, 861–863. 10.1038/13158. [PubMed: 10491603]

Giorgio A, Watkins KE, Chadwick M, James S, Winmill L, Douaud G, De Stefano N, Matthews PM, Smith SM, Johansen-Berg H, James AC, 2010. Longitudinal changes in grey and white matter during adolescence. Neuroimage 49, 94–103. 10.1016/j.neuroimage.2009.08.003. [PubMed: 19679191]

Giorgio A, Watkins KE, Douaud G, James AC, James S, De Stefano N, Matthews PM, Smith SM, Johansen-Berg H, 2008. Changes in white matter microstructure during adolescence. Neuroimage 39, 52–61. 10.1016/j.neuroimage.2007.07.043. [PubMed: 17919933]

Hammelrath L, Škokić S, Khmelinskii A, Hess A, van der Knaap N, Staring M, Lelieveldt BPF, Wiedermann D, Hoehn M, 2016. Morphological maturation of the mouse brain: an in vivo MRI and histology investigation. Neuroimage 125, 144–152. 10.1016/j.neuroimage.2015.10.009. [PubMed: 26458518]

Herting MM, Maxwell EC, Irvine C, Nagel BJ, 2012. The impact of sex, puberty, and hormones on white matter microstructure in adolescents. Cerebr. Cortex 22, 1979–1992. 10.1093/cercor/bhr246.

Hill RA, Li AM, Grutzendler J, 2018. Lifelong cortical myelin plasticity and age-related degeneration in the live mammalian brain. Nat. Neurosci 21, 683–695. 10.1038/s41593-018-0120-6. [PubMed: 29556031]

Ho TC, Colich NL, Sisk LM, Oskirko K, Jo B, Gotlib IH, 2020. Sex differences in the effects of gonadal hormones on white matter microstructure development in adolescence. Developmental Cognitive Neuroscience 42, 100773. 10.1016/j.dcn.2020.100773. [PubMed: 32452463]

Jenkinson M, Beckmann CF, Behrens TEJ, Woolrich MW, Smith SM, 2012. FSL. Neuroimage 62, 782–790. 10.1016/j.neuroimage.2011.09.015. [PubMed: 21979382]

Jernigan TL, Stiles J, 2017. Construction of the human forebrain. WIREs Cogn Sci 8, e1409. 10.1002/wcs.1409.

Karlsgodt KH, John M, Ikuta T, Rigoard P, Peters BD, Derosse P, Malhotra AK, Szeszko PR, 2015. The accumbofrontal tract: diffusion tensor imaging characterization and developmental change from childhood to adulthood. Hum. Brain Mapp 36, 4954–4963. 10.1002/hbm.22989. [PubMed: 26366528]

Kennedy KM, Erickson KI, Rodrigue KM, Voss MW, Colcombe SJ, Kramer AF, Acker JD, Raz N, 2009. Age-related differences in regional brain volumes: a comparison of optimized voxel-based morphometry to manual volumetry. Neurobiol. Aging 30, 1657–1676. 10.1016/j.neurobiolaging.2007.12.020. [PubMed: 18276037]

Kiely M, Triebswetter C, Cortina LE, Gong Z, Alsameen MH, Spencer RG, Bouhrara M, 2022. Insights into human cerebral white matter maturation and degeneration across the adult lifespan. Neuroimage 247, 118727. 10.1016/j.neuroimage.2021.118727. [PubMed: 34813969]

Koss WA, Lloyd MM, Sadowski RN, Wise LM, Juraska JM, 2015. Gonadectomy before puberty increases the number of neurons and glia in the medial prefrontal cortex of female, but not male, rats. Dev. Psychobiol 57, 305–312. 10.1002/dev.21290. [PubMed: 25782706]

Lebel C, Beaulieu C, 2011. Longitudinal development of human brain wiring continues from childhood into adulthood. J. Neurosci 31, 10937–10947. 10.1523/JNEUROSCI.5302-10.2011. [PubMed: 21795544]

Lebel C, Caverhill-Godkewitsch S, Beaulieu C, 2010. Age-related regional variations of the corpus callosum identified by diffusion tensor tractography. Neuroimage 52, 20–31. 10.1016/j.neuroimage.2010.03.072. [PubMed: 20362683]

Lebel C, Deoni S, 2018. The development of brain white matter microstructure. Neuroimage 182, 207–218. 10.1016/j.neuroimage.2017.12.097. [PubMed: 29305910]

Lenroot RK, Gogtay N, Greenstein DK, Wells EM, Wallace GL, Clasen LS, Blumenthal JD, Lerch J, Zijdenbos AP, Evans AC, Thompson PM, Giedd JN, 2007. Sexual dimorphism of brain developmental trajectories during childhood and adolescence. Neuroimage 36, 1065–1073. 10.1016/j.neuroimage.2007.03.053. [PubMed: 17513132]

Liu YH, Kundu R, Wu L, Luo W, Ignelzi MA, Snead ML, Maxson RE, 1995. Premature suture closure and ectopic cranial bone in mice expressing Msx2 transgenes in the developing skull. Proc. Natl. Acad. Sci. U.S.A 92, 6137–6141. 10.1073/pnas.92.13.6137. [PubMed: 7597092]

Mack CM, Fitch RH, Cowell PE, Schrott LM, Denenberg VH, 1993. Ovarian estrogen acts to feminize the female rat's corpus callosum. Dev. Brain Res 71, 115–119. 10.1016/0165-3806(93)90112-N. [PubMed: 8431995]

Markham JA, Morris JR, Juraska JM, 2007. Neuron number decreases in the rat ventral, but not dorsal, medial prefrontal cortex between adolescence and adulthood. Neuroscience 144, 961–968. 10.1016/j.neuroscience.2006.10.015. [PubMed: 17137726]

Mirsalis JC, 1995. Transgenic models for detection of mutations in tumors and normal tissues of rodents. Toxicol. Lett 82 (83), 131–134. 10.1016/0378-4274(95)03472-2. [PubMed: 8597040]

Pfefferbaum A, Kwon D, Brumback T, Thompson WK, Cummins K, Tapert SF, Brown SA, Colrain IM, Baker FC, Prouty D, De Bellis MD, Clark DB, Nagel BJ, Chu W, Park SH, Pohl KM, Sullivan EV, 2018. Altered brain developmental trajectories in adolescents after initiating drinking. Aust. J. Pharm 175, 370–380. 10.1176/appi.ajp.2017.17040469.

Pfefferbaum A, Rohlfing T, Pohl KM, Lane B, Chu W, Kwon D, Nolan Nichols B, Brown SA, Tapert SF, Cummins K, Thompson WK, Brumback T, Meloy MJ, Jernigan TL, Dale A, Colrain IM, Baker FC, Prouty D, De Bellis MD, Voyvodic JT, Clark DB, Luna B, Chung T, Nagel BJ, Sullivan EV, 2016. Adolescent development of cortical and white matter structure in the NCANDA sample: role of sex, ethnicity, puberty, and alcohol drinking. Cerebr. Cortex 26, 4101–4121. 10.1093/cercor/bhv205.

Pfefferbaum A, Rohlfing T, Rosenbloom MJ, Chu W, Colrain IM, Sullivan EV, 2013. Variation in longitudinal trajectories of regional brain volumes of healthy men and women (ages 10 to 85years) measured with atlas-based parcellation of MRI. Neuroimage 65, 176–193. 10.1016/j.neuroimage.2012.10.008. [PubMed: 23063452]

Pfefferbaum A, Sullivan EV, Carmelli D, 2004. Morphological changes in aging brain structures are differentially affected by time-linked environmental influences despite strong genetic stability. Neurobiol. Aging 25, 175–183. 10.1016/s0197-4580(03)00045-9. [PubMed: 14749135]

Pfefferbaum A, Sullivan EV, Carmelli D, 2001. Genetic regulation of regional microstructure of the corpus callosum in late life. Neuroreport 12, 1677–1681. 10.1097/00001756-200106130-00032. [PubMed: 11409738]

Pfefferbaum A, Sullivan EV, Swan GE, Carmelli D, 2000. Brain structure in men remains highly heritable in the seventh and eighth decades of life. Neurobiol. Aging 21, 63–74. 10.1016/s0197-4580(00)00086-5. [PubMed: 10794850]

Piekarski DJ, Boivin JR, Wilbrecht L, 2017a. Ovarian hormones organize the maturation of inhibitory neurotransmission in the frontal cortex at puberty onset in female mice. Curr. Biol 27, 1735–1745.e3. 10.1016/j.cub.2017.05.027. [PubMed: 28578932]

Piekarski DJ, Johnson CM, Boivin JR, Thomas AW, Lin WC, Delevich K, Galarce EM, Wilbrecht L, 2017b. Does puberty mark a transition in sensitive periods for plasticity in the associative neocortex? Brain Res 1654, 123–144. 10.1016/j.brainres.2016.08.042. [PubMed: 27590721]

Piekarski DJ, Zahr NM, Zhao Q, Sullivan EV, Pfefferbaum A, 2022. Alcohol's effects on the mouse brain are modulated by age and sex. Addiction Biol 27 10.1111/adb.13209.

Pohl KM, Sullivan EV, Rohlfing T, Chu W, Kwon D, Nichols BN, Zhang Y, Brown SA, Tapert SF, Cummins K, Thompson WK, Brumback T, Colrain IM, Baker FC, Prouty D, De Bellis MD, Voyvodic JT, Clark DB, Schirda C, Nagel BJ, Pfefferbaum A, 2016.

Harmonizing DTI measurements across scanners to examine the development of white matter microstructure in 803 adolescents of the NCANDA study. Neuroimage 130, 194–213. 10.1016/j.neuroimage.2016.01.061. [PubMed: 26872408]

Rohlfing T, Maurer CR Jr., 2003. Nonrigid image registration in shared-memory multiprocessor environments with application to brains, breasts, and bees. IEEE transactions on information technology in biomedicine : a publication of the IEEE Engineering in Medicine and Biology Society 7, 16–25. [PubMed: 12670015]

Rohlfing T, Zahr NM, Sullivan EV, Pfefferbaum A, 2010. The SRI24 multichannel atlas of normal adult human brain structure. Hum. Brain Mapp 31, 798–819. 10.1002/hbm.20906. [PubMed: 20017133]

Safaiyan S, Kannaiyan N, Snaidero N, Brioschi S, Biber K, Yona S, Edinger AL, Jung S, Rossner MJ, Simons M, 2016. Age-related myelin degradation burdens the clearance function of microglia during aging. Nat. Neurosci 19, 995–998. 10.1038/nn.4325. [PubMed: 27294511]

Schmithorst VJ, Holland SK, Dardzinski BJ, 2008. Developmental differences in white matter architecture between boys and girls. Hum. Brain Mapp 29, 696–710. 10.1002/hbm.20431. [PubMed: 17598163]

Simmonds DJ, Hallquist MN, Asato M, Luna B, 2014. Developmental stages and sex differences of white matter and behavioral development through adolescence: a longitudinal diffusion tensor imaging (DTI) study. Neuroimage 92, 356–368. 10.1016/j.neuroimage.2013.12.044. [PubMed: 24384150]

Slater DA, Melie-Garcia L, Preisig M, Kherif F, Lutti A, Draganski B, 2019. Evolution of white matter tract microstructure across the life span. Hum. Brain Mapp 40, 2252–2268. 10.1002/hbm.24522. [PubMed: 30673158]

Smith SM, Jenkinson M, Woolrich MW, Beckmann CF, Behrens TEJ, Johansen-Berg H, Bannister PR, De Luca M, Drobnjak I, Flitney DE, Niazy RK, Saunders J, Vickers J, Zhang Y, De Stefano N, Brady JM, Matthews PM, 2004. Advances in functional and structural MR image analysis and implementation as FSL. Neuroimage 23 (Suppl. 1), S208–S219. 10.1016/j.neuroimage.2004.07.051 . [PubMed: 15501092]

Song S-K, Sun S-W, Ju W-K, Lin S-J, Cross AH, Neufeld AH, 2003. Diffusion tensor imaging detects and differentiates axon and myelin degeneration in mouse optic nerve after retinal ischemia. Neuroimage 20, 1714–1722. 10.1016/j.neuroimage.2003.07.005. [PubMed: 14642481]

Song S-K, Yoshino J, Le TQ, Lin S-J, Sun S-W, Cross AH, Armstrong RC, 2005. Demyelination increases radial diffusivity in corpus callosum of mouse brain. Neuroimage 26, 132–140. 10.1016/j.neuroimage.2005.01.028. [PubMed: 15862213]

Sousa SS, Amaro E, Crego A, Gonçalves ÓF, Sampaio A, 2018. Developmental trajectory of the prefrontal cortex: a systematic review of diffusion tensor imaging studies. Brain Imaging and Behavior 12, 1197–1210. 10.1007/s11682-017-9761-4. [PubMed: 28913594]

Sowell ER, Thompson PM, Toga AW, 2004. Mapping changes in the human cortex throughout the span of life. Neuroscientist 10, 372–392. 10.1177/1073858404263960. [PubMed: 15271264]

Sturrock RR, 1980. Myelination of the mouse corpus callosum. Neuropathol. Appl. Neurobiol 6, 415–420. 10.1111/j.1365-2990.1980.tb00219.x. [PubMed: 7453945]

Sullivan EV, Adalsteinsson E, Sood R, Mayer D, Bell R, McBride W, Li T-K, Pfefferbaum A, 2006. Longitudinal brain magnetic resonance imaging study of the alcohol-preferring rat. Part I: adult brain growth. Alcohol Clin. Exp. Res 30, 1234–1247. 10.1111/j.1530-0277.2006.00145.x. [PubMed: 16792572]

Sullivan EV, Lane B, Kwon D, Meloy MJ, Tapert SF, Brown SA, Colrain IM, Baker FC, De Bellis MD, Clark DB, Nagel BJ, Pohl KM, Pfefferbaum A, 2017. Structural brain anomalies in healthy adolescents in the NCANDA cohort: relation to neuropsychological test performance, sex, and ethnicity. Brain Imaging and Behavior 11, 1302–1315. 10.1007/s11682-016-9634-2. [PubMed: 27722828]

Sullivan EV, Pfefferbaum A, Swan GE, Carmelli D, 2001. Heritability of hippocampal size in elderly twin men: equivalent influence from genes and environment. Hippocampus 11, 754–762. 10.1002/hipo.1091. [PubMed: 11811670]

Sullivan EV, Rohlfing T, Pfefferbaum A, 2010. Quantitative fiber tracking of lateral and interhemispheric white matter systems in normal aging: relations to timed performance. Neurobiol. Aging 31, 464–481. 10.1016/j.neurobiolaging.2008.04.007. [PubMed: 18495300]

Tamnes CK, Østby Y, Fjell AM, Westlye LT, Due-Tønnessen P, Walhovd KB, 2010. Brain maturation in adolescence and young adulthood: regional age-related changes in cortical thickness and white matter volume and microstructure. Cerebr. Cortex 20, 534–548. 10.1093/cercor/bhp118.

Ventura-Antunes L, Mota B, Herculano-Houzel S, 2013. Different scaling of white matter volume, cortical connectivity, and gyrification across rodent and primate brains. Front. Neuroanat 7 10.3389/fnana.2013.00003.

Westlye LT, Walhovd KB, Dale AM, Bjornerud A, Due-Tonnessen P, Engvig A, Grydeland H, Tamnes CK, Ostby Y, Fjell AM, 2010. Life-Span changes of the human brain white matter: diffusion tensor imaging (DTI) and volumetry. Cerebr. Cortex 20, 2055–2068. 10.1093/cercor/bhp280.

White HE, Goswami A, Tucker AS, 2021. The intertwined evolution and development of sutures and cranial morphology. Front. Cell Dev. Biol 9, 653579 10.3389/fcell.2021.653579. [PubMed: 33842480]

Wilkinson CC, Stence NV, Serrano CA, Graber SJ, Batista-Silverman L, Schmidt-Beuchat E, French BM, 2020. Fusion patterns of major calvarial sutures on volume-rendered CT reconstructions. J. Neurosurg. Pediatr 25, 519–528. 10.3171/2019.11.PEDS1953.

Yeatman JD, Wandell BA, Mezer AA, 2014. Lifespan maturation and degeneration of human brain white matter. Nat. Commun 5, 4932. 10.1038/ncomms5932. [PubMed: 25230200]

Zahr NM, Sullivan EV, Pohl KM, Pfefferbaum A, 2021. Age differences in brain structural and metabolic responses to binge ethanol exposure in Fisher 344 rats. Neuropsychopharmacology 46, 368–379. 10.1038/s41386-020-0744-6. [PubMed: 32580206]

Zhang B, Cory E, Bhattacharya R, Sah R, Hargens AR, 2013. Fifteen days of microgravity causes growth in calvaria of mice. Bone 56, 290–295. 10.1016/j.bone.2013.06.009. [PubMed: 23791778]

Zhang K, Sejnowski TJ, 2000. A universal scaling law between gray matter and white matter of cerebral cortex. Proc. Natl. Acad. Sci. USA 97, 5621–5626. 10.1073/pnas.090504197. [PubMed: 10792049]

Zhao Q, Sullivan EV, Honnorat N, Adeli E, Podhajsky S, De Bellis MD, Voyvodic J, Nooner KB, Baker FC, Colrain IM, Tapert SF, Brown SA, Thompson WK, Nagel BJ, Clark DB, Pfefferbaum A, Pohl KM, 2021. Association of heavy drinking with deviant fiber tract development in frontal brain systems in adolescents. JAMA Psychiatr 78, 407–415. 10.1001/jamapsychiatry.2020.4064.

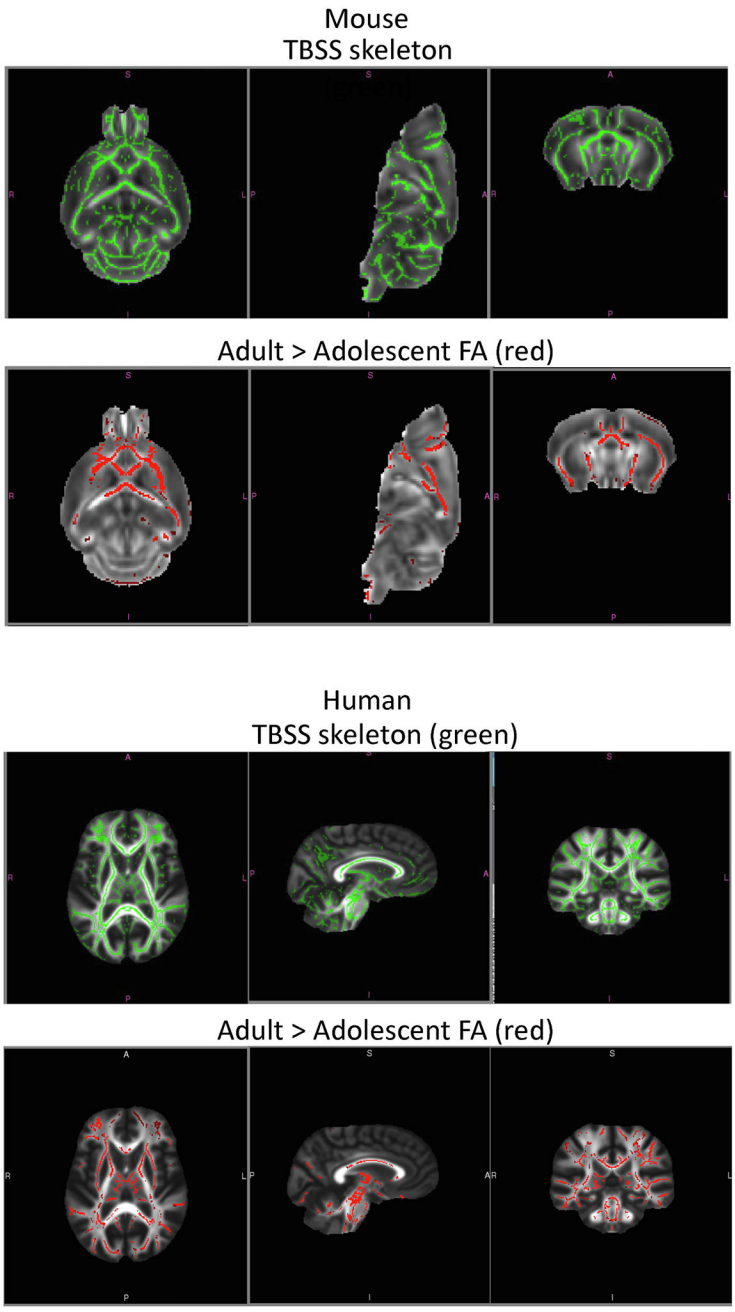

Fig. 1.

TBSS skeletons for both mice (top) and humans (bottom) are presented in green. In red, the results of permutation testing showing voxels in which young adult mice or humans have higher FA than their early-adolescent counterparts.

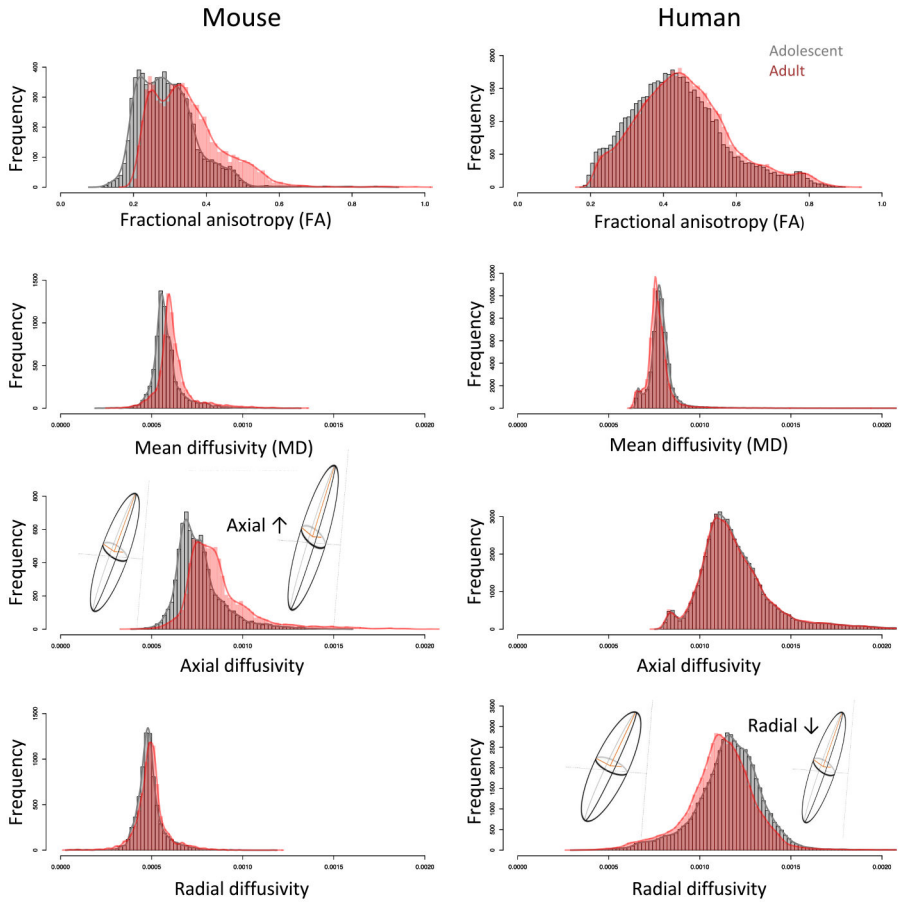

Fig. 2.

Mouse (left column) and human (right column) showing overlapping distributions of water diffusion indices. In both mice and humans, adults showed significantly higher fractional anisotropy (FA) compared with adolescents (row 1). However, species differed in underlying mechanism, with greater age-related axial diffusivity driving this effect in mice (row 3) but lower radial diffusivity driving this affect in older humans (row 4). Ellipsoid models showing age related differences in axial diffusivity in mice and radial diffusivity in humans present a schematic representation for the observed differences in water diffusion. Fig. 3 top: Mouse: Upper left—Adult mice had significantly larger white matter volumes than adolescent mice. Upper middle—White matter volume as a function of total brain volume for adolescents (gray) and adults (black). The across-group regression across all mice is dashed gray. Upper right—white matter volumes after regression on total brain volume. Note that the adult-adolescence difference endured after adjustment for total brain volume.

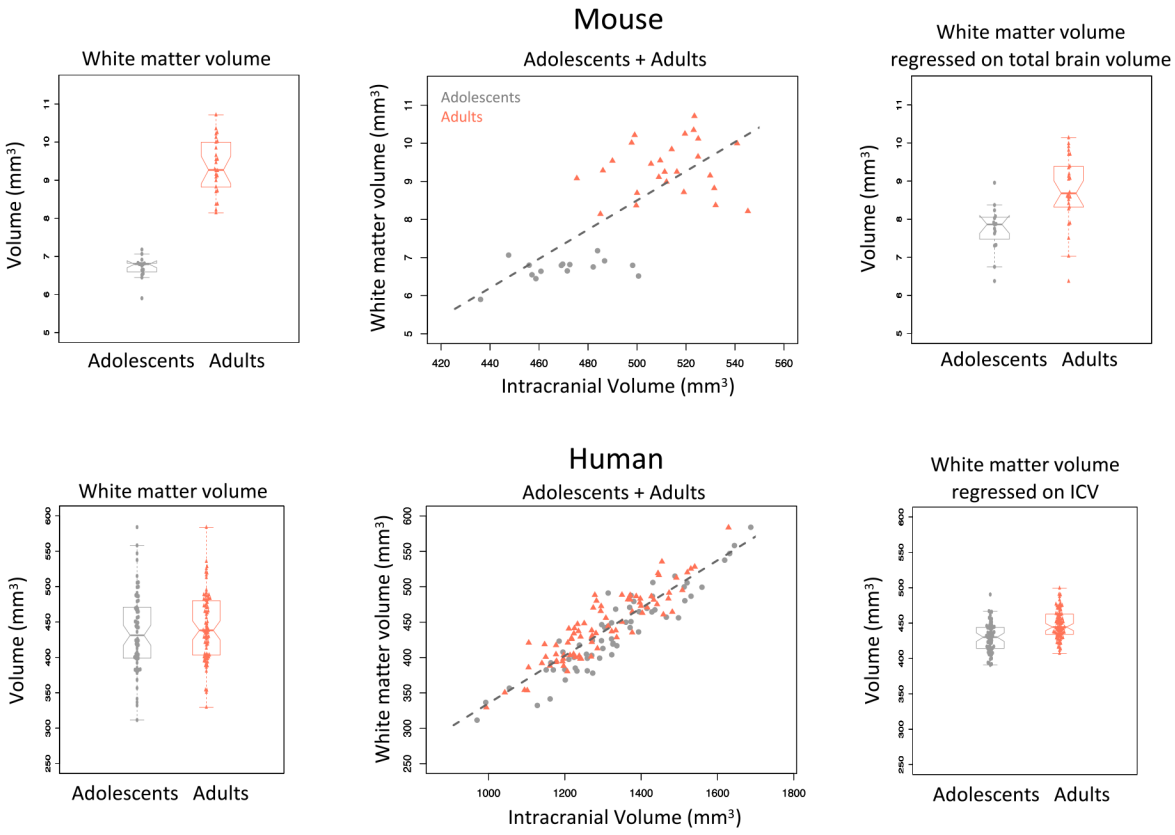

Fig. 3.

Top: Mouse: Upper left—Adult mice had significantly larger white matter volumes than adolescent mice. Upper middle—White matter volume as a function of total brain volume for adolescents (gray) and adults (red). The across-group regression across all mice is dashed gray. Upper right—white matter volumes after regression on total brain volume. Note that the adult-adolescence difference endured after adjustment for total brain volume. Bottom: Human: Lower left—Adolescents and adults did not differ in white matter volume. Lower middle—White matter volume as a function of total brain volume across all participants, with adolescents in gray and adults in red and across all participant regression in dashed gray. Lower right—white matter volumes after regression on total intracranial volume (ICV). Note that an adult-adolescence difference manifest after adjustment for ICV.

Table 1

Demographic information of the NCANDA youth.

			Site			Race			
Age group	**N**	**Age (mean ± SD)**	**SRI**	**Duke**	**UCSD**	**Asian**	**Black**	**Caucasian**	**Other**
Adolescents									
Male	31	12.6 (.33)	11	7	13	3	1	25	2
Female	31	12.6 (.33)	9	10	12	3	8	19	1
Young adults									
Male	38	20.4 (.28)	3	10	25	4	5	28	1
Female	43	20.5 (.31)	4	17	22	3	15	25	0

Table 2

DTI metrics statistics for mouse (top) and human (bottom).

Mouse		**Adolescents**		**Adults**					
DTI metric	**N**	**Mean**	**SD**	**N**	**Mean**	**SD**	**t**	**df**	**p**
FA	15	0.2943	0.0192	24	0.3495	0.0117	10.057	20.55	**2.18E-09**
MD	15	0.000581	2.07E-05	24	0.000621	2.71E-05	5.222	35.39	**7.95E-06**
AD	15	0.000765	2.68E-05	24	0.000867	3.09E-05	10.873	33.09	**1.84E-12**
RD	15	0.000487	2.07E-05	24	0.000497	2.60E-05	1.292	34.69	0.2048
Human		**Adolescents**		**Adults**					
DTI metric	**N**	**Mean**	**SD**	**N**	**Mean**	**SD**	**t**	**df**	**p**
FA	62	0.4384	0.0130	81	0.4573	0.0119	8.9174	125.10	**4.85E-15**
MD	62	0.000786	1.45E-05	81	0.000770	1.58E-05	−6.2301	136.40	**5.42E-09**
AD	62	0.001197	1.73E-05	81	0.001194	1.89E-05	−0.8804	136.31	0.3802
RD	62	0.000581	1.65E-05	81	0.000558	1.67E-05	−7.9778	132.32	**6.23E-13**

Bold font = significant difference: adult > adolescent.